Journal of Tropical Forest Science 37(3): 329–341 (2025)
https://doi.org/10.26525/jtfs2025.37.3.329
ISSN: 0128-1283, eISSN: 2521-9847

ANTI-ANGIOGENIC EFFECT OF 9-METHOXYCANTHIN-6-ONE ISOLATED FROM *EURYCOMA LONGIFOLIA* ON ENDOTHELIAL CELL LINE

Nor Datiakma MA[1, 2], Nurhanan MY[1], Nor Jannah S[1] & Mohd Nazri I[2, 3, *]

[1]*Natural Products Division, Forest Research Institute Malaysia, 52109 Kepong, Selangor, Malaysia*
[2]*Analytical Biochemistry Research Centre, Universiti Sains Malaysia, 11900, Bayan Lepas, Pulau Pinang, Malaysia*
[3]*Institute for Research in Molecular Medicine, Universiti Sains Malaysia, 11800, USM, Pulau Pinang, Malaysia*

**mdnazri@usm.my*

Submitted December 2024; accepted February 2025

Eurycoma longifolia Jack has been traditionally used in Southeast Asia for various ailments including cancer. Its bioactive quassinoids exhibit significant pharmacological properties. Among them, 9-methoxycanthin-6-one shows potential anti-cancer activity. However, its anti-angiogenic effects remain unexplored. This study evaluates its anti-angiogenic effects on EA.hy926 endothelial cells. Three assays (spheroid growth, tube formation, and cell migration) were performed, and data were analysed using one-way ANOVA with Dunnett's test ($p < 0.0001$). Results show that 9-methoxycanthin-6-one inhibited EA.hy926 proliferation (IC_{50}: 25.85 ± 1.29 µM) compared to suramin (IC_{50}: 60.94 ± 5.03 µM). In the spheroid assay, it significantly reduced spheroid diameter (88.73% at $IC_{50}/8$ to 82.63% at IC_{50}) at 48 hours, though inhibition at 96 hours was inconsistent, suggesting possible adaptive responses. No tube formation was observed at $IC_{50}/2$ and IC_{50} after 6 and 18 hours. At lower concentrations ($IC_{50}/8$ to $IC_{50}/4$), tube length (93.84–134.75 µm) and width (17.77–20.65 µm) were significantly reduced. Cell migration was also inhibited (61.26 ± 8.05% at $IC_{50}/8$ to 19.19 ± 8.64% at IC_{50}) compared to NT (100%). Overall, 9-methoxycanthin-6-one exhibits significant anti-angiogenic potential supporting its role as an angiogenesis inhibitor in multiple in vitro models.

Keywords: 9-methoxycanthin-6-one, *Eurycoma longifolia*, anti-angiogenesis, spheroid growth, tube formation, cell migration

INTRODUCTION

Cancer remains a significant global health challenge with incidence and mortality rates continuing to rise. According to the latest Global Cancer Statistics, an estimated 19.3 million new cancer cases and nearly 10 million cancer-related deaths occurred worldwide in 2020 (Sung et al. 2021). The most prevalent types include lung, breast, colorectal, and prostate cancers, influenced by genetic, environmental, and lifestyle factors (Ferlay et al. 2024). Despite advances in treatments, cancer is still remains a leading cause of death due to its complexity and resistance mechanisms. The development of newer cancer drugs, including targeted therapies and immunotherapies has significantly improved patient outcomes. This offers more effective and less toxic alternatives to traditional chemotherapy (Ramos et al. 2021) such as cisplatin (Rajadurai et al. 2020). The newer cancer drugs such as imatinib (Cohen et al. 2021) and immunotherapy drugs such as Nivolumab (Gong et al. 2018) have revolutionised cancer treatment. However, challenges remain in terms of accessibility and affordability of these advanced therapies. Thus, ongoing research and investment in novel therapeutics are essential to address the growing cancer burden.-

The progression of cancer relies heavily on angiogenesis, the formation of new blood vessels from existing ones. This process is crucial for monitoring and detecting cancer. It begins with a tumour growing because of cells multiplying uncontrollably and surpassing apoptosis (Shchors & Evan 2007, Yoo & Kwon 2013). As the tumour grows, it loses oxygen and nutrients, releasing angiogenic factors like the Vascular Endothelial Growth Factor (VEGF). These new blood vessels supply the tumour with oxygen

and nutrients, aiding its growth and spread (Carmeliet & Jain 2000, Dudley & Griffioen 2023). The new capillary network supports tumour expansion and cancer cell metastasis, thus playing an essential role in determining the stage and prognosis of cancer (Eichholz et al. 2010).

Given the challenges associated with conventional treatments, researchers have turned to herbal-based drug development as a promising alternative in cancer therapy. The development of newer anti-cancer drugs from herbal sources has gained significant attention due to the diverse bioactive compounds found in medicinal plants. Many modern cancer treatments have originated from natural sources, including paclitaxel from *Taxus brevifolia* and vinblastine from *Catharanthus roseus*, demonstrating the potential of plant-derived compounds in oncology (Nasim et al. 2022). Herbal-derived compounds exhibit multiple anti-cancer properties, including apoptosis induction, angiogenesis inhibition, and immune system modulation, making them valuable candidates for novel drug development. For instance, curcumin from *Curcuma longa* has shown promising results in inhibiting cancer cell proliferation and enhancing chemotherapy efficacy (Sharifi-Rad et al. 2020). Similarly, epigallocatechin gallate (EGCG) from green tea (*Camellia sinensis*) has been explored for its ability to target cancer cell survival pathways (Tauber et al. 2020). Beyond their direct cytotoxic effects, these herbal compounds play a crucial role in combination therapies, enhancing the effectiveness of existing treatments while reducing toxicity. Given the rising concerns over drug resistance and adverse effects associated with conventional chemotherapy, ongoing research into herbal compounds offers a promising avenue for developing safer and more effective cancer therapies. As a result, the integration of herbal-derived agents into cancer drug development has emerged as a critical strategy for expanding therapeutic

Many studies have shown that medicinal plants can inhibit cancer progression, and their traditional use in treating various diseases is now being validated by modern scientific research (Siddiqui et al. 2022). One plant of interest is *Eurycoma longifolia* Jack (Simaroubaceae), or Long Jack. *E. longifolia* is a popular herbal supplement widely known for its aphrodisiac properties (Jayusman et al. 2017, Nazirah et al. 2018). Research shows that *E. longifolia* supplementation can increase testosterone levels, particularly in men with hypogonadism (Leisegang et al. 2022). Its proven benefits reinforce its commercial value and widespread use in traditional and modern medicine as a natural aphrodisiac. Beyond its well-known aphrodisiac effects, *E. longifolia* has gained attention for its diverse bioactive compounds, including quassinoids, alkaloids, triterpenes, and steroidal compounds, which are found predominantly in its roots (Nurhanan et al. 2005). These compounds exhibit various biological activities, such as antimicrobial, antiparasitic, and notably, anti-cancer properties (Nurhanan et al. 2005, Rehman et al. 2016). Many studies have shown that medicinal plants, including *E. longifolia*, can inhibit cancer progression, and their traditional uses are now being validated by modern scientific research (Siddiqui et al. 2022). With increasing interest in plant-based therapeutics, ongoing research into *E. longifolia* continues to explore its potential beyond reproductive health, particularly in oncology and other medical applications.

We have previously identified 9-methoxycanthin-6-one activities on a panel of cancer cell lines such as ovarian, breast, colorectal, cervical, and skin cancer (Nor Datiakma et al. 2021, Nurhanan et al. 2022). Additionally, there are reports of its activity against lung cancer (Kuo et al. 2004), melanoma and fibro sarcoma (Kardono et al. 1991). Despite these findings, the anti-angiogenic activity of 9-methoxycanthin-6-one has yet to be explored. Therefore, this study is conducted to evaluate the anti-angiogenesis activities of 9-methoxycanthin-6-one on endothelial cells (EA.hy926) via three anti-angiogenic assays, namely spheroid growth, tube formation and cell migration.

MATERIALS AND METHODS

Materials and chemicals

The endothelial cell EA.hy926 (ATCC® CRL 926) was purchased from the American Type

Culture Collection (ATCC, Manassas, VA, USA). Ovarian cancer cell A2780 was purchased from the European Collection of Authenticated Cell Cultures (ECACC, Salisbury, UK). Endothelial EA.hy926 cells were kindly supplied by EMAN Biodiscoveries Sdn. Bhd, Sungai Petani, Kedah, Malaysia. Dulbecco's Modified Eagle's medium (DMEM), foetal bovine serum, gentamicin, agarose, and methyl cellulose were purchased from Sigma-Aldrich, St. Louis, MO, USA. Penicillin-streptomycin and amphotericin B were purchased from Sigma-Aldrich, USA. Matrigel was obtained from Corning (Lowell, MA, USA).

Plant compound 9-methoxycanthin-6-one

Compound 9-methoxycanthin-6-one (Figure 1) was isolated from the root of *E. longifolia* based on the method of Nurhanan et al. (2022). Briefly, 9-Methoxycanthin-6-one was extracted from *E. longifolia* hairy root culture using Soxhlet extraction with chloroform at 35–45 °C for 16 hours. The extract was then filtered, concentrated under reduced pressure, and subjected to silica gel column chromatography for purification. Gradient elution using n-hexane:DCM and DCM:methanol was employed to obtain the purified compound. The crude extract was further fractionated using silica gel 60 column chromatography with gradient elution of n-hexane:DCM (9:1, 7:3, 3:7, 1:9), yielding seven distinct fractions (FR1–FR7). Fractions FR1–FR3 were pooled and subjected to re-chromatography using silica gel with n-hexane:DCM and DCM:methanol, leading to the isolation of 9-methoxycanthin-6-one as a yellow amorphous powder. The structural identity of the compound was confirmed through electron ionization mass spectrometry (EIMS), as well as ^{1}H and ^{13}C nuclear magnetic resonance (NMR) spectroscopy, with spectral data consistent with previously reported findings.

Cell culture

Frozen EA.hy926 cells from cryovial was thawed at room temperature and immediately transferred to a 25 cm^2 flask containing 4 mL complete media to dilute the cryoprotectant (DMSO). The flask was then incubated at 37 °C in a 5% carbon dioxide atmosphere. The media consisted of Dulbecco's Modified Eagle's medium (DMEM), 10% fetal bovine serum, 1% penicillin-streptomycin, 1% gentamicin and 1% amphotericin B. After 6 hours or when most cells had adhered to the flask surface, media containing diluted cryoprotectant were discarded and replaced with fresh media. Again, the flask was incubated at 37 °C in a 5% carbon dioxide atmosphere. Once the cells reached 70-80% confluence (covering 70-80% of the flask surface), they were subcultured; the cells were washed twice with sterile phosphate buffered saline (PBS, pH 7.4), detached using 1x trypsin, and fresh media was added. The subculture ratio was 1:3. Experiments were conducted after passage 3. Ovarian A2780 cancer cells were cultured using the same method and utilised in the co-culture spheroid formation assay.

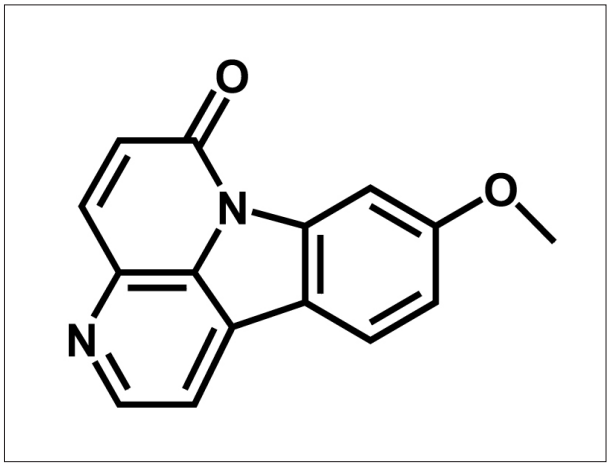

Figure 1 Structure of 9-methoxycanthine-6-one

EA.hy926 cell viability assay

A 100 µL of cells suspension were seeded into each well of a 96-well plate at a density of 6000 cells per well and allowed to grow for 24 hours. The following formula was used to calculate the required volume (V1) to achieve a density of 6000 cells per well:

$$V_1 = \frac{M_2 \times V_2}{M_1}$$

$$\text{Volume to seed, } V_1 = \frac{60000 \text{ cells/mL} \times 10 \text{ mL per 96-well plate}}{\text{Cell count in suspension, cells mL}^{-1} \text{ (detached from flask)}}$$

where M_1 = Cell count in suspension, V_1 = Volume to seed, M_2 = Total cells needed and V_2 = Required volume in 100 µL per well of 96-well plate.

Cells were then treated with 9-methoxycanthin-6-one and suramin, a standard angiogenesis inhibitor (Crew et al. 1996). After 72 hours, cell viability was assessed using the Sulforhodamine B (SRB) assay, following the methods described by Nurhanan et al. (2017), which was modified from Skehan et al. (1990). Fifty (50) microliters of ice-cold tricholoroacetic acid (TCA) was added into each well of 96–well plate and incubated for 30 min at room temperature before washing with tap water. To stain the living cells, 100 µL of 0.4% SRB was added to each well for 30 min and then rinsed with 1% acetic acid. 100 µL of Tris buffer was added to each well for solubilisation. The optical density (OD) of treated and non-treated cells was measured at 492 nm using a Magellan V 7.5 microtiter plate reader (Tecan, Switzerland). Cell viability was estimated: [OD_{492nm} of treated cells/ (cells/ OD_{492nm} of non-treated cells) × 100].

The IC_{50} values were determined from the dose-response curve of the percentage of cell viability versus the concentration of the compounds (µM). The cell viability assay for each treatment was performed in triplicate in at least three independent experiments, and the IC_{50} values are given as the mean ± SEM. These values served as a baseline for evaluating the potency of the compounds in anti-angiogenic assays, as referenced by (Drevs & Schneider 2006, Reynolds 2010, Kaya-Tilki et al. 2024).

Anti-angiogenesis assays

Anti-spheroid growth assay (Co-culture)

Spheroids used in this assay were generated by the hanging-drop method described by Kelm et al. (2003). An anti-spheroids growth assay was performed as described by Bayat et al. (2018) with slight modification. For spheroids formation, EA.hy926 and A2780 were prepared separately at a cell density of 1×10^4 cell mL^{-1} each. The cells were then mixed in media containing Dulbecco's Modified Eagle Medium (DMEM), 10% fetal bovine serum, 1% penicillin-streptomycin, 1% gentamicin and 2% methylcellulose. The mixtures of cells were dispensed in drops of 25 µL onto the lids of 150 mm culture plate using a multichannel pipette. The cover was inverted over sterile water and incubated with culture condition: 37°C; 5% CO_2 until spheroids growth was observed. Prior to treatments of 9-methoxycanthin-6-one and suramin on spheroids, 48-well plates were coated with 1.5% agarose and left to solidify. A serial dilution of the compounds ranging from IC_{50} to $IC_{50/8}$ was prepared in DMEM. The IC_{50} value was obtained based on the results of the SRB assay conducted on EA.hy926. 400 µL of the diluted compounds were added to each well, followed by transferring one spheroid into each well. The spheroids were incubated, and images were captured under an inverted microscope with 40X magnification at 0, 48 and 96 hours of incubation. The images were captured under the light microscope (Olympus CKX41) at 40X magnification using ToupView x64 (ver. 3.7.9229.20170607) image analyser software (ToupTek, Hangzhou, China). Suramin was used as a positive control in this study. For analysis, spheroids' diameters were calculated using ImageJ 1.53t (http://imagej. nih.gov/ij/) software. The results were presented as average ± SE (n = 3).

Anti-tube formation assay

Tube formation assay was performed as described by Chan et al. (2015). Initially, 100 µL of EAhy.926 (10×10^5 cells mL^{-1}) were seeded into a 48-well plate coated with 150 µL of Matrigel matrix (Corning, USA), followed by treatment with a medium containing compounds at a

Table 1 The IC_{50} value of 9-methoxycanthin-6-one and suramin

No	Compound	Molecular weight ($g\ mol^{-1}$)	IC_{50} value (μM)
1	9-methoxycanthin-6-one	250.25	25.85 ± 1.29
2	Suramin	1429.17	60.94 ± 5.03

50% serial dilution of concentration from IC_{50} to $IC_{50/8}$. Tube formation was observed at 6- and 18 hours post-treatment. The formation of tube-like structures was visualized, and images were captured under the light microscope (Olympus CKX41) at 40X magnification using ToupView x64 (ver. 3.7.9229.20170607) image analyser software (ToupTek, Hangzhou, China). Tube formation was determined by measuring the length and width of tubes formed in each well using ImageJ 1.53t software and the percentage of tube formation (length and width) was then calculated. The results were showed as an average ± SE (n=3) (Carpentier et al. 2020).

Anti-cell migration assay

Cell migration assay was performed as described by Al-Salahi et al (2013). EA.hy926 was plated in a 48-well plate in DMEM until at least 90% confluent monolayer growth was obtained. The monolayer was uniformly and vertically scratched using a sterile 10 μL micropipette tip. Wells were then treated with 9-methoxycanthin-6-one with concentrations ranging from IC50 to IC50/8. The scratch was observed at 0 (T0) and 24 (T24) hours under an inverted microscope with 40X magnification and the images were captured under the light microscope (Olympus CKX41) at 40X magnification using ToupView x64 (ver. 3.7.9229.20170607) image analyser software (ToupTek, Hangzhou, China). Images were then analysed using ImageJ 1.53t software and the percentage of cell migration inhibition was then calculated relative to zero time using the formula:

$$\text{Cell migration inhibition} = 100 - \frac{(\text{the width of gap at } T_0 - \text{the width of gap at } T_{24})}{\text{the width of gap at } T_0} \times 100$$

where T_0 = cell migration at 0-hour and T_{24} = cell migration at 24-hour. Suramin was used as a positive control in this study. The results were presented as the mean percentage of migration inhibition to the control ± SE (n = 9).

Statistical analysis

The differences in spheroid diameter, tube formation and cell migration between the treated and non-treated groups were analysed using one-way analysis of variance (ANOVA), followed by Dunnett's test (Prism version 5.0, Graphpad Software). A difference with $p < 0.05$ is considered statistically significant.

RESULTS

Inhibition of EA.hy926 cell proliferation

Since angiogenesis involves the local proliferation of endothelial cells in response to an angiogenic stimulus (Cárdenas et al. 2011), we first tested whether 9-methoxycanthin-6-one could suppress the proliferation of EA.hy926. The result showed that 9-methoxycanthin-6-one inhibited EA.hy926 proliferation with an IC_{50} value of 25.85 ± 1.29 μM. The control drug suramin had an IC_{50} value of 60.94 ± 5.03 μM, showing that 9-methoxycanthin-6-one was more effective inhibiting cell proliferation (Table 1).

Inhibition of spheroid growth

The spheroid growth assay was used in this study to assess anti-angiogenic properties because of its ability to mimic the three-dimensional structure of tumours in the human body. This test provides insight into how anti-angiogenesis agents impact tumour growth, the formation of new blood vessels and the spread of cancer cells through the bloodstream, which are crucial for cancer growth and survival (Thakuri et al. 2016).

Figure 2 shows the inhibition of spheroids growth. The photomicrograph displays an anti-spheroid growth activity of 9-methoxycanthin-

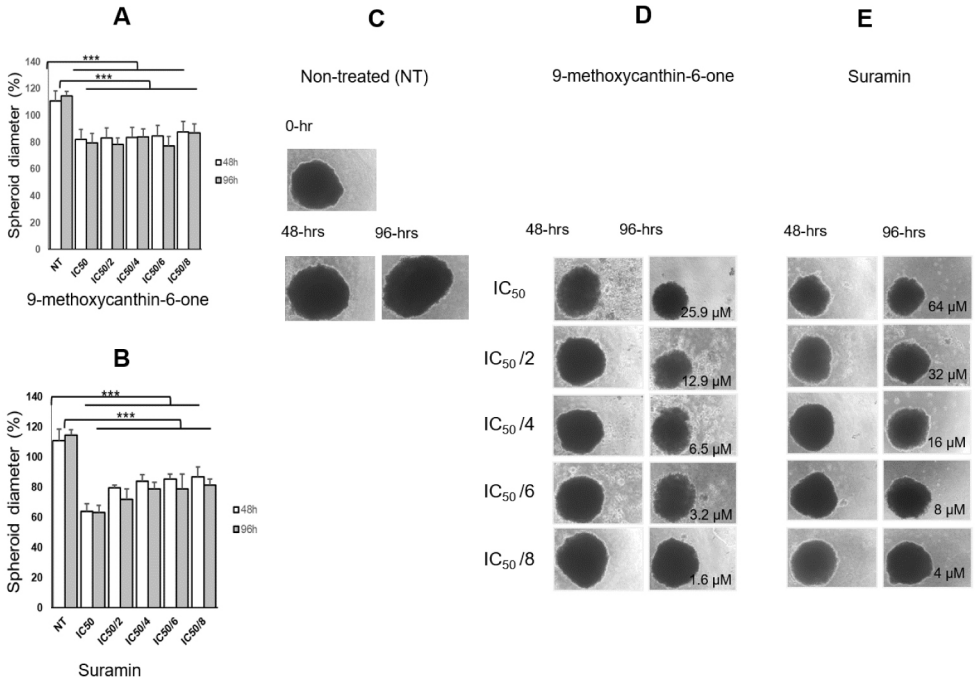

Figure 2 Inhibition of spheroid growth. The photomicrograph showed an anti-spheroid growth activity of 9-methoxycanthin-6-one and suramin (standard drug). The analysis was conducted by measuring the diameter of spheroids after incubation at 48- and 96-hours with respective compounds

Figure 2A and 2B The bar charts represent the percent change in spheroid diameter across different concentrations of the compounds over the two incubation periods. The non-treated group (NT) shows a consistent increase in spheroid diameter while treatments result in a reduction, particularly at higher concentrations

Figure 2C Photomicrographs of non-treated spheroids serve as a negative control. The images depict how spheroids in non-treated samples showed an increment in diameters and continued to increase after 96 hours

Figure 2D and 2E Photomicrograph images show the effect of 9-methoxycanthin-6-one and suramin on spheroids growth in a dose-dependent manner. At 48 hours, the trend of spheroids growth inhibition decreased as the concentration of compounds increased. However, at 96 hours, the trend of spheroid growth inhibition was not consistent in 9-methoxycanthin-6-one- treated spheroids. This may indicate that the spheroids had adapted to the treatments or undergone changes in response to the longer time treatment of 9-methoxycanthin-6-one. Data represent mean ± SD, $***p < 0.0001$

6-one and suramin. Size measurements of the spheroids predict the efficacy of 9-methoxycanthin-6-one treatment. During the first 48 hours, non-treated spheroids showed an increase in diameter, showing normal growth. In contrast, spheroids treated with 9-methoxycanthin-6-one and suramin showed significant growth inhibition, with a decrease in spheroid diameter as the concentration of the compounds increased. However, after 96 hours of incubation, spheroids treated with 9-methoxycanthin-6-one showed inconsistent growth inhibition, while those treated with suramin did not which is suggesting possible adaptation to treatment.

Inhibition of EA.hy926 tube formation

The results from the photomicrograph in Figure 3 show the tube formation inhibitory activity of 9-methoxycanthin-6-one and suramin. This experiment measures the ability of these compounds to inhibit EA.hy926 tube formation. Tube formation in non-treated samples (Figure 2A) can be observed when the lumen (loop) containing tubules appears after 6 hours of

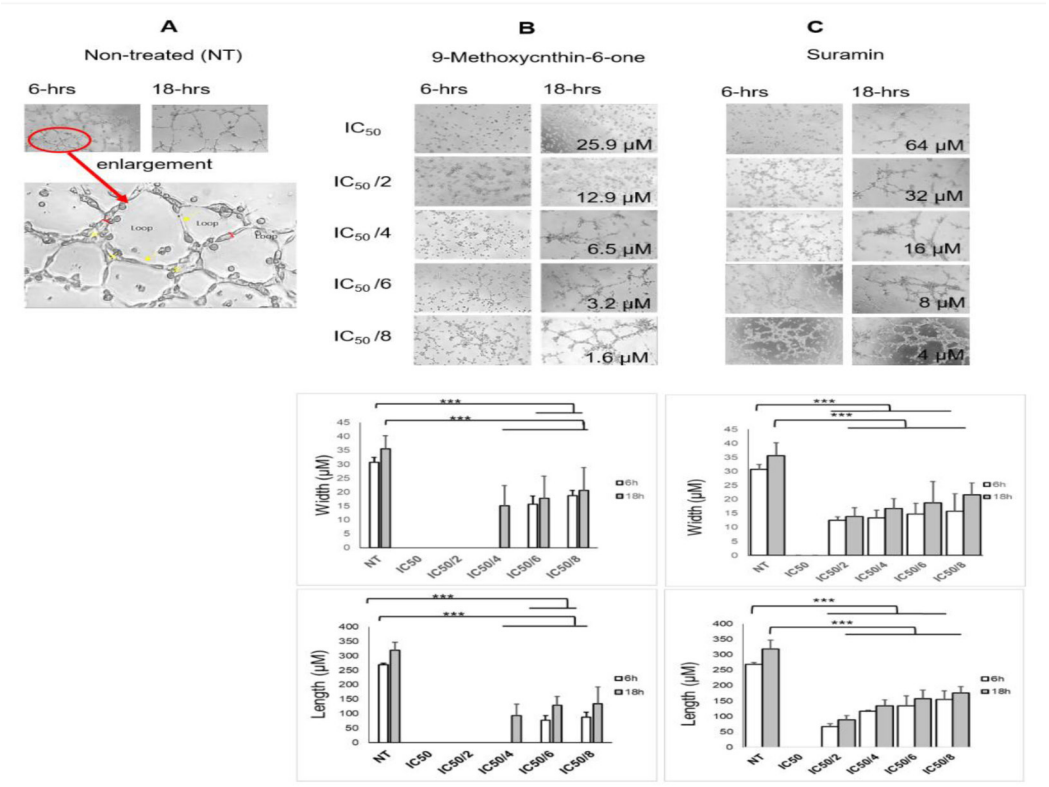

Figure 3 Tube formation of EC EA.hy926. The analysis was conducted by measuring the width and length of tubes formed at 6- and 18 hours of incubation with respective compounds. Photomicrograph showing the effects of 9-methoxycanthin-6-one and suramin on EC EA.hy926

Figure 3A Photomicrographs of non-treated EC EA.hy926 serve as a negative control. The images depict how cells grown on matrigel media differentiated into branching morphogenesis, resulting in capillary tube-like structures made up of numerous cells with intercellular gaps or lumens. The enlarged photomicrograph (Figure 1(A)) clearly shows the tube's width (red bracket), tubes (yellow arrow), loops (lumens) and branching points (+). The length of tubes was determined by measuring the length of the tubes between two branching points. Tube formations were observed at 6 hours of incubation, and the width and length of the tubes were increased after 18 hours of incubation

Figure 3B and 3C Photomicrograph images show the effect of 9-methoxycanthin-6-one and suramin on EA.hy926 tube's formation in dose-dependent manner. The tube formation length and width were increased as dosages of compounds decreased. Results were statistically evaluated using one-way ANOVA followed by Dunnett's test, ***$p < 0$

EA.hy926 cell incubation, representing a network of tube formation. The bar chart illustrates the dose-dependent inhibitory effect of 9-methoxycanthin-6-one and suramin on the length and width of EA.hy926 capillary-like structures.

In the non-treated sample, endothelial cell EA.hy926 tubes began to form after 6 hours of incubation. By 18 hours of incubation, these initial tube networks had merged, resulting in a denser structure with more lumens. Although the number of lumens decreased by 18 hours, the width and length of the tubes increased.

Treatments of 9-methoxycanthin-6-one and suramin resulted in reduced tube formation compared to non-treated samples. The effect of 9-methoxycanthin-6-one on endothelial cell EA.hy926 (Figure 2B) revealed no tube formation at concentrations ranging from 12.9 to 25.9 µM after 6 and 18 hours of incubation. At 6-hour incubation time, tube formation formed at lower concentrations (1.6 to 3.2 µM), with increased width and length observed after 18 hours. However, tube formation in endothelial cell EA.hy926- treated with 9-methoxycanthin-6-one remained lower than in non-treated samples.

Treatment with suramin resulted in a

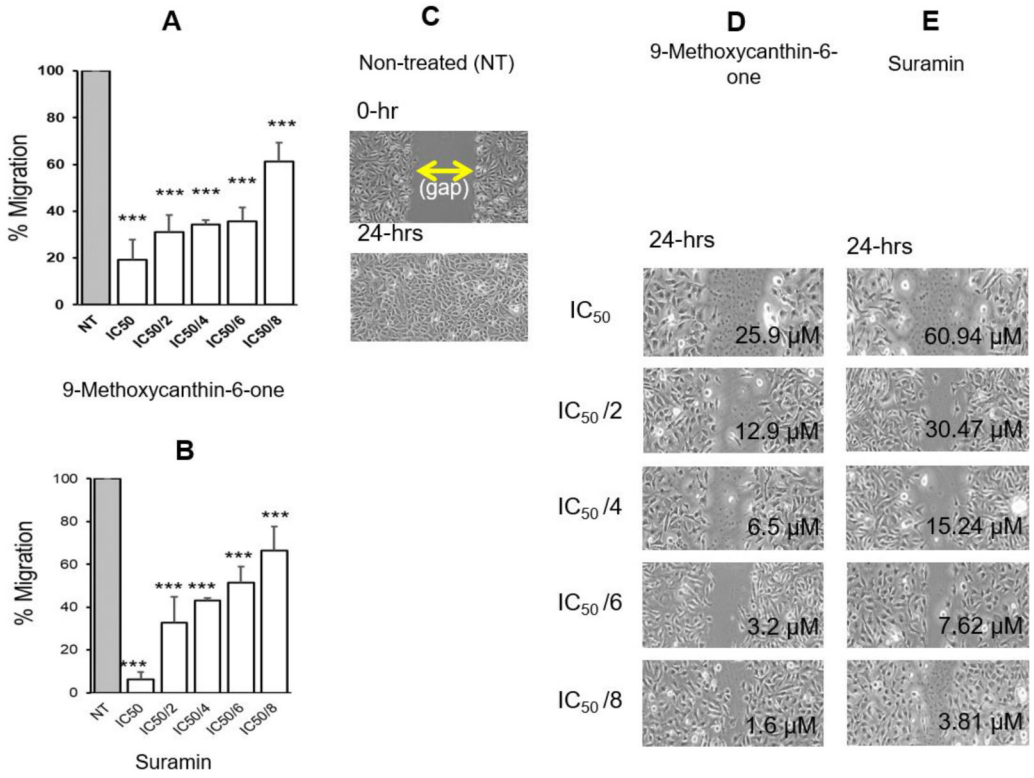

Figure 4 EC EA.hy926 migration. The analysis was conducted by measuring the width of gap between the cells and by comparing the width at 24- over 0-hour of incubation

Figure 4A and 4B The bar charts represent the percentage of cell migration after treatment with varying concentrations of 9-methoxycanthin-6-one and suramin. Both compounds demonstrate a dose-dependent reduction in migration, with lower concentrations resulting in increased migration while higher concentrations lead to significant inhibition

Figure 4C The photomicrographs of non-treated EC EA.hy926 cells serve as a control and showing complete cell migration within 24 hours. The initial gap (highlighted with a yellow arrow) closes as the cells move to fill the space

Figure 4D and 4E The inhibition of EC EA.hy926 migration after treatment with 9-methoxycanthin-6-one and suramin were showing a significant EC EA.hy926 migration inhibitory effect in a dose-dependent manner. This is evident from the representative images in the photomicrographs where treated samples show fewer migrating cells and reduced cell movement toward the gap area as compared to non-treated samples. Data are shown as mean ± SD, ***$p < 0.0001$

reduced tube formation of EA.hy926 in a dose dependent manner. Tube formation was absent at 64 µM after 6- and 18-hours of incubation. Tubes formed at concentrations ranging from 4 to 32 µM after 6- and 18-hours of incubation, with increased width and length observed after 18-hours of incubation.

Inhibition of cell EA.hy926 migration

The photomicrographs in Figure 4 illustrate the anti-migration activity of 9-methoxycanthin-6-one and suramin, a standard drug, on endothelial EA.hy926 cell. This experiment measures their ability to inhibit cell migration, a critical factor in cancer progression. Cell migration is evaluated by measuring the closure of a gap introduced at 0 hour and after 24 hours. In the photomicrograph, non-treated EA.hy926 cells showed 0% migration inhibition after 24-hrs incubation. Conversely, EA.hy926 cells treated with 9-methoxycanthin-6-one showed concentration-dependent inhibition of cell migration, with higher concentrations resulting in more pronounced inhibition. This effect is visually evident by the larger remaining

gaps compared to the control. A similar trend was observed with suramin, where increasing concentrations led to increased inhibition of cell migration, as showed by the percentage of migration inhibition.

DISCUSSION

Cancer initiation involves the transformation of normal cells into cancerous ones that proliferate uncontrollably, forming early-stage avascular tumours reliant on nearby tissue for nutrients and oxygen through diffusion. As the tumour grows, its metabolic demands increase and creating a hypoxic environment within the tumour mass. This hypoxia triggers the angiogenic switch, which marks the onset of angiogenesis (Zhao & Adjei 2015). Tumour cells then release pro-angiogenic factors such as vascular endothelial growth factor (VEGF), stimulating the growth of new blood vessels from existing ones (Li et al. 2012). In response to these signals, endothelial cells from nearby blood vessels proliferate and migrate toward the tumour. These endothelial cell degrade the surrounding extracellular matrix and forming sprouts that extend into the hypoxic tumour region. Over time, these sprouting endothelial cells connect to form tubular structures and create new blood vessels that penetrate the tumour. This complex process is regulated by multiple signalling pathways, involving VEGF, fibroblast growth factor (FGF), and platelet-derived growth factor (PDGF). These newly formed blood vessels supply the tumour with essential nutrients and oxygen that is crucial for its growth and survival (Naumov et al. 2006).

There is limited information on the anti-angiogenic effects of 9-methoxycanthin-6-one. However, a related study by Al-Salahi et al. (2013) reported the anti-angiogenic potential of a partially purified quassinoid-rich fraction from *E. longifolia* root extract in the proliferation, migration, and differentiation of human umbilical vein endothelial cells (HUVECs). To our knowledge, this is the first report on the anti-angiogenesis activity of 9-methoxycanthin-6-one from *E. longifolia*. This novel discovery emphasises the potential of this compound as a therapeutic agent in cancer treatments that target angiogenesis. The results show consistent dose-dependent inhibition of multiple angiogenic pathways, offering new insights into the potential medical applications of a compound derived from traditional medicinal knowledge.

Before conducting anti-angiogenesis studies, the endothelial EA.hy926 cell proliferation assay was performed to determine the IC_{50} value for each compound, including suramin as a positive control. Suramin is widely used as a positive control in anti-angiogenic assays due to its well-documented ability to inhibit angiogenesis by targeting multiple growth factor pathways. It effectively blocks vascular endothelial growth factor (VEGF), basic fibroblast growth factor (bFGF), and platelet-derived growth factor (PDGF) (Kakuguchi et al. 2018, Parveen et al. 2020), all of which are critical for endothelial cell proliferation, migration, and tube formation. These mechanisms make suramin a reliable reference compound for evaluating the anti-angiogenic effects of new compounds. Additionally, its dose-dependent inhibition of endothelial cell proliferation and capillary-like tube formation has been validated in multiple studies, ensuring consistent and reproducible results in angiogenesis research.

A proliferation assay was performed on the endothelial cell line EA.hy926 to determine the IC_{50} value, which served as the baseline concentration for subsequent anti-angiogenesis assays. This approach ensured that the anti-angiogenic effects of 9-methoxycanthin-6-one and suramin were not due to cytotoxicity. In this study, 9-methoxycanthin-6-one was found to inhibit multiple stages of angiogenesis significantly, including endothelial cell proliferation, spheroid growth, tube formation, and migration (Nassar et al. 2011).

The co-culture spheroid growth assay, in which ovarian cancer cells (A2780) and endothelial cells (EA.hy926) were co-cultured, allowed us to mimic real tumour environments. Cancer cells secrete growth factors such as VEGF which stimulate endothelial cells to start angiogenesis (Wu et al. 2021). The co-culture spheroid growth model allowed these two cell types to interact and form spheroids that mimic real tumours in the body (Sonoda et al. 2003). This more realistic model enabled a precise study of the dynamic interactions between cancer and endothelial cells (Li et al. 2021). In this context, both cancer and endothelial

cells could engage in processes that closely resemble in vivo environments, making this model crucial for evaluating the effectiveness of 9-methoxycanthin-6-one. In the co-culture spheroid growth assay (Figure 2) results showed that spheroid growth inhibition increased with higher concentrations of 9-methoxycanthin-6-one and suramin after 48 hours compared to untreated spheroids. The reduction in spheroid diameter indicates suppressed angiogenesis. This reduction impaired endothelial cell proliferation and restricted nutrient supply essential for sustained tumour-like growth in vitro. However, by 96 hours, the inhibition trend of spheroid growth became inconsistent in those treated with 9-methoxycanthin-6-one. This suggests that spheroids may have adapted or responded differently to prolonged treatment. The initial inhibition trend followed by inconsistent results over time implies potential changes in molecular pathways that could affect long-term efficacy (Thakuri et al. 2019).

Treatment with 9-methoxycanthin-6-one significantly increased the inhibition of tube formation in endothelial cell EA.hy926 compared to suramin. In non-treated cells, extensive tube formation was observed over 18 hours, characterized by robust tubular structures with increased width and length, indicative of natural endothelial cell behaviour without inhibitory agents (Figure 3). Treatment with 9-methoxycanthin-6-one and suramin reduced the number of lumens and weakened the bridges within the tube-like structures, resulting in narrower and thinner tubes. This substantial inhibition highlights the potent anti-angiogenic effect on endothelial cells from 9-methoxycanthin-6-one, preventing endothelial cell EA.hy926 cells from undergoing the morphological changes necessary for tube formation. The significant reduction in tube formation with 9-methoxycanthin-6-one treatment also suggests that the compound disrupts the endothelial cell interactions required for angiogenesis. Additionally, the tube formation assay allows both quantitative and qualitative analysis of angiogenic and anti-angiogenic factors, making it a valuable tool for screening such agents.

The study results also show that 9-methoxycanthin-6-one exhibits significant anti-migration activity on endothelial cell EA.hy926, suggesting its potential as a potent inhibitor of cancer angiogenesis. Cell migration is crucial in cancer progression as it allows cancer cells to invade new areas and metastasize. In our study, higher concentrations of 9-methoxycanthin-6-one led to greater inhibition of cell migration, as shown by larger gaps remaining after 24 hours compared to non-treated samples (Figure 4). The inhibition of migration further emphasises the compound's potential to prevent cancer cell spread, a key aspect of its therapeutic relevance.

These results provide compelling evidence of the dose-dependent anti-angiogenic activities of 9-methoxycanthin-6-one across several consistent assays. Spheroid growth represents 3D tumour growth, tube formation models capillary formation, and cell migration mimics the motility needed for metastasis. Together, these findings support the conclusion that 9-methoxycanthin-6-one is a promising agent for inhibition of cancer angiogenesis.

As this is the first study to report the anti-angiogenic effects of 9-methoxycanthin-6-one on endothelial cells, further research is critical to explain its underlying modes of action. Comparatively, eurycomanone from *E. longifolia* has been reported to influence the mTOR signalling pathway, which is critical in regulating cell growth, proliferation, and survival. By suppressing autophagy and angiogenesis, eurycomanone inhibits cancer cell proliferation and impairs processes essential for tumour growth and metastasis (Ye et al. 2022). These findings highlight the therapeutic potential of *E. longifolia*-derived compounds and underscore the need for further exploration of 9-methoxycanthin-6-one to identify its specific molecular targets and applications in anti-cancer therapy.

In addition to its promising anti-angiogenic properties, 9-methoxycanthin-6-one satisfies key criteria for drug development, including Lipinski's Rule of Five (RoF), which is commonly used to assess a compound's potential for oral bioavailability. With a molecular weight of 250.25 g mol^{-1}, 9-methoxycanthin-6-one adheres to one of the critical criteria of Lipinski's Rule, which suggests a better likelihood of membrane permeability and absorption (Kerns & Di 2016, Nurhanan et al. 2023). A low molecular weight improves a compound's ability to pass through biological membranes, facilitating absorption

and systemic circulation (Veber et al. 2002). Furthermore, the compound's lipophilicity and other properties warrant further exploration to determine its suitability as a therapeutic agent in clinical settings.

CONCLUSION

Plant compound 9-methoxycanthin-6-one effectively inhibits angiogenesis in EA.hy926 endothelial cells. This was demonstrated through its ability to inhibit spheroid growth, tube formation, and cell migration in a dose-dependent manner. The results offer significant new insights into the therapeutic potential of this bioactive compound derived from traditional medicinal knowledge in cancer treatments targeting angiogenesis. However, the varying effects of 9-methoxycanthin-6-one over extended periods in the spheroid growth assay suggest that further validation is necessary to understand its long-term efficacy. Future studies also should focus on validating these findings in vivo and investigating the underlying molecular mechanisms via the multi-omics approach.

ACKNOWLEDGEMENT

This research was funded by the development fund under the 12th Malaysian plan (grant number 24-01070-2001) by the Government of Malaysia. The authors are grateful to Mrs. Ruzana Rabuzin for assisting in the cell culture activities.

REFERENCES

Al-Salahi OSA, Kit-Lam C et al. 2013. Anti-angiogenic quassinoid-rich fraction from *Eurycoma longifolia* modulates endothelial cell function. *Microvascular Research* 90: 30–39.

Bayat N, Izadpanah R, Ebrahimi-Barough S el al. 2018. The anti-angiogenic effect of atorvastatin in glioblastoma spheroids tumor cultured in fibrin gel: In 3D in vitro model. *Asian Pacific Journal of Cancer Prevention* 19: 2553–2560. https://doi.org/10.22034/APJCP.2018.19.9.2553

Cardenas C, Quesada AR & Medina MA. 2011. Anti-angiogenic and anti-inflammatory properties of kahweol, a coffee diterpene. *PLoS ONE* 6: 1–9. https://doi.org/10.1371/journal.pone.0023407

Carmeliet P & Jain RK. 2000. Angiogenesis in cancer and other diseases. *Nature* 407: 249–257. https://doi.org/10.1038/35025220

Carpentier G, Berndt S, Ferratge S el al. 2020. Angiogenesis Analyzer for ImageJ — A comparative morphometric analysis of "Endothelial Tube Formation Assay" and "Fibrin Bead Assay." *Scientific Reports* 10: 1–13.

Chan YK, Zhang H, Liu P el al. 2015. Proteomic analysis of exosomes from nasopharyngeal carcinoma cell identifies intercellular transfer of angiogenic proteins. *International Journal of Cancer* 137: 1830–1841.

Cohen P, Cross D & Janne PA. 2021. Kinase drug discovery 20 years after imatinib: progress and future directions. *Nature Reviews Drug Discovery* 20: 551–569. https://doi.org/10.1038/s41573-021-00195-4

Crew JP, O'brien TS, Harris AL. 1996. Bladder cancer angiogenesis, its role in recurrence, stage progression and as a therapeutic target. *Cancer and Metastasis Reviews* 15: 221–230. https://doi.org/10.1007/BF00437475

Drevs J & Schneider V. 2006. The use of vascular biomarkers and imaging studies in the early clinical development of anti-tumour agents targeting angiogenesis. *Journal of Internal Medicine* 260: 517–529.

Dudley AC & Griffioen AW. 2023. Pathological angiogenesis: mechanisms and therapeutic strategies. *Angiogenesis* 26: 313–347. https://doi.org/10.1007/s10456-023-09876-7

Eichholz A, Merchant S & Gaya AM. 2010. Anti-angiogenesis therapies: Their potential in cancer management. *Onco Targets and Therapy* 3: 69–82.

Ferlay J, Ervik MF, Lam F el al. 2024. *Global Cancer Observatory: Cancer Today.* WHO-International Agency for Research on Cancer. https://doi.org/10.1002/ijc.33588

Gong J, Chehrazi-Raffle A, Reddi S & Salgia R. 2018. Development of PD-1 and PD-L1 inhibitors as a form of cancer immunotherapy: A comprehensive review of registration trials and future considerations. *Journal for ImmunoTherapy of Cancer* 6: 1–18. https://doi.org/10.1186/s40425-018-0316-z

Jayusman PA, Mohamed IN, Thu HE & Shuid AN. 2017. Effect of *Eurycoma longifolia* on Sexual Behavior in Sexually Dysfunctional Male: a Systematic Review. *International Journal of Pharmacy and Pharmaceutical Sciences* 9: 46–52. https://doi.org/10.22159/ijpps.2017v9i12.21812

Kakuguchi W, Nomura T, Kitamura T el al. 2018. Suramin, screened from an approved drug library, inhibits HuR functions and attenuates malignant phenotype of oral cancer cells. *Cancer Medicine* 7: 6269–6280. ay el al., 2021https://doi.org/10.1002/cam4.1877

Kardono LBS, Angerhofer CK, Tsauri S, Padmawinata K, Pezzuto JM & Douglas Kinghorn A. 1991. Cytotoxic and antimalarial constituents of the roots of *Eurycoma longifolia. Journal of Natural Products* 54: 1360–1367.

Kaya-Tilki E, Ozturk AA, Engür-Ozturk S & Dikmen M. 2024. Enhanced anti-angiogenic effects of aprepitant-loaded nanoparticles in human umbilical vein endothelial cells. *Scientific Reports* 14: 1–17. https://doi.org/10.1038/s41598-024-70791-y

Kelm JM, Timmins NE, Brown CJ, Fussenegger M & Nielsen LK. 2003. Method for generation of homogeneous multicellular tumor spheroids applicable to a wide variety of cell types. *Biotechnology and Bioengineering* 83: 173–180.

Kerns EH & Di L. Drug-Like Properties Concepts, Structure, Design, And Methods From Adme To Toxicity Optimization. 2016. Academic Press, Cambridge MA.

Kuo PC, Damu AG, Lee KH & Wu TS. 2004. Cytotoxic and antimalarial constituents from the roots of *Eurycoma longifolia*. *Bioorganic and Medicinal Chemistry* 12: 537–544.

Leisegang K, Finelli R, Sikka SC, Panner & Selvam MK. 2022. *Eurycoma longifolia* (Jack) Improves Serum Total Testosterone in Men: A Systematic Review and Meta-Analysis of Clinical Trials. *Medicina* 58: 1047. https://doi.org/10.3390/medicina58081047

Li WW, Li VW, Hutnik M & Chiou AS. 2012. Tumor angiogenesis as a target for dietary cancer prevention. *Journal of Oncology* 2012: 1–23.

Li Z, Yan-Qing W, Xiao Y el al. 2021 Exosomes secreted by chemoresistant ovarian cancer cells promote angiogenesis. *Journal of Ovarian Research* 14: 1–7.

Nasim N, Sandeep IS & Mohanty S. 2022. Plant-derived natural products for drug discovery: current approaches and prospects. *Nucleus (India)* 65: 399–411. https://doi.org/10.1007/s13237-022-00405-3

Nassar ZD, Aisha AFA, Ahamed MBK el al. 2011. Antiangiogenic properties of Koetjapic acid, a natural triterpene isolated from *Sandoricum koetjaoe Merr*. *Cancer Cell International* 11: 1–8. https://doi.org/10.1186/1475-2867-11-12

Naumov GN, Akslen LA & Folkman J. 2006. Role of angiogenesis in human tumor dormancy: Animal models of the angiogenic switch. *Cell Cycle* 5: 1779–1787.

Nazirah A, Nor-Hasnida H, Ismanizan I el al. 2018. Production of 9-methoxycanthin-6-one in elicited *Eurycoma longifolia* hairy root. *Journal of Tropical Forest Science* 30: 606–614. https://doi.org/10.26525/jtfs2018.30.4.606614

Nurhanan MY, Nor Datiakma MA, Jauri MH, Ling SK, Hassan NH & Sallehuddin NJ. 2022. The In Vitro Anti-Cancer Activities and Mechanisms of Action of 9-methoxycanthin-6-one from *Eurycoma longifolia* in Selected Cancer Cell Lines. *Molecules* 27: 1–18.

Nurhanan MY, Hawariah LPA, Ilham AM & Shukri MAM. 2005. Cytotoxic effects of the root extracts of *Eurycoma longifolia* Jack. *Phytotherapy Research* 19: 994–996.

Nurhanan MY, Nor Azah MA, Zunoliza A, Siti Humeriah AG, Siti Syarifah MM & Nor Hayati A. 2017. In vitro anticancer activity and high-performance liquid chromatography profiles of *Aquilaria subintegra* fruit and seed extracts. *Journal of Tropical Forest Science* 29: 208–214.

Nurhanan MY, Wahab HA, Al-Thiabat MG, Sallehudin NJ & Jauri MH. 2023. In Vitro and In Silico Analysis of the Anticancer Effects of Eurycomanone and Eurycomalactone from *Eurycoma longifolia*. *Plants* 12: 1–20. https://doi.org/10.3390/plants12152827

Nor Datiakma M, Nurhanan MY, Muhammad Haffiz J & Norjannah S. 2021. Proteome profile of ovarian cancer cell line A2780 treated with 9-methoxycanthin-6-one from *Eurycoma longifolia*. *Malaysian Journal of Biochemistry and Molecular Biology* 1: 92–99.

Parveen N, Lin YL, Khan MI, Chou RH, Sun CM & Yu C. 2020. Suramin derivatives play an important role in blocking the interaction between FGF1 and FGFRD2 to inhibit cell proliferation. *European Journal of Medicinal Chemistry* 206: 112656.

Rajadurai P, How SH, Liam CK, Sachithanandan A, Soon SY & Tho LM. 2020. Lung Cancer in Malaysia. *Journal of Thoracic Oncology* 15: 317–323. https://doi.org/10.1016/j.jtho.2019.10.021

Ramos A, Sadeghi S & Tabatabaeian H. 2021. Battling chemoresistance in cancer: Root causes and strategies to uproot them. *International Journal of Molecular Sciences* 22: 1–22. https://doi.org/10.3390/ijms22179451

Rehman SU, Choe K & Yoo HH. 2016. Review on a traditional herbal medicine, *Eurycoma longifolia* Jack (Tongkat Ali): Its traditional uses, chemistry, evidence-based pharmacology, and toxicology. *Molecules* 21: 1–31.

Reynolds AR. 2010. Potential relevance of bell-shaped and U-shaped dose-responses for the therapeutic targeting of angiogenesis in cancer. *Dose-Response* 8: 253–284.

Sharifi-Rad J, Rayess Yel, Rizk AA el al. 2020. Turmeric and Its Major Compound Curcumin on Health: Bioactive Effects and Safety Profiles for Food, Pharmaceutical, Biotechnological and Medicinal Applications. *Frontiers in Pharmacology* 11: 1–23. https://doi.org/10.3389/fphar.2020.01021

Shchors K & Evan G. 2007. Tumor angiogenesis: Cause or consequence of cancer? *Cancer Research* 67: 7059–7061.

Siddiqui Aj, Jahan S, Singh R el al. 2022. Plants in anticancer drug discovery: From molecular mechanism to chemoprevention. *Biomedical Research International* 2022: 1–18.

Skehan P, Storeng R, Scudiero D el al. 1990. New colorimetric cytotoxicity assay for anticancer-drug screening. *Journal of the National Cancer Institute* 82: 1107–1112.

Sonoda T, Kobayashi H, Kaku T, Hirakawa T & Nakano H. 2003. Expression of angiogenesis factors in monolayer culture, multicellular spheroid, and in vivo transplanted tumor by human ovarian cancer cell lines. *Cancer Letters* 196: 229–237.

Sung H, Ferlay J, Siegel RL el al. 2021. Global Cancer Statistics 2020: GLOBOCAN Estimates of Incidence and Mortality Worldwide for 36 Cancers in 185 Countries. *CA: A Cancer Journal for Clinicians* 71: 209–249. https://doi.org/10.3322/caac.21660

Tauber AL, Schweiker SS & Levonis SM. 2020. From tea to treatment; epigallocatechin gallate and its potential involvement in minimizing the metabolic changes in cancer. *Nutrition Research* 74: 23–36. https://doi.org/10.1016/j.nutres.2019.12.004

Thakuri PS, Gupta M, Plaster M & Tavana H. 2019.

Quantitative size-based analysis of tumor spheroids and responses to therapeutics. *Assay and Drug Development Technologies* 17: 140–149.

Thakuri PS, Ham SL, Luker GD & Tavana H. 2016. Multiparametric analysis of oncology drug screening with aqueous two-phase tumor spheroids. *Molecular Pharmaceutics* 13: 3724–3735.

Veber DF, Johnson SR, Cheng HY, Smith BR., Ward KW & Kopple KD.2002. Molecular properties that influence the oral bioavailability of drug candidates. *Journal of Medicinal Chemistry* 45: 2615–2623. https://doi.org/10.1021/jm020017n

Wu Y, Gao J & Liu X. 2021. Deregulation of angiopoietin-like 4 slows ovarian cancer progression through vascular endothelial growth factor receptor 2 phosphorylation. *Cancer Cell International* 21: 1–15.

Ye G, Xu M, Shu Y el al. 2022. A quassinoid diterpenoid eurycomanone from *Eurycoma longifolia* Jack exerts anti-cancer effect through autophagy inhibition. *Molecules* 27: 4398. https://doi.org/10.3390/molecules27144398

Yoo SY & Kwon SM. 2013. Angiogenesis and its therapeutic opportunities. *Mediators of Inflammation* 2013: 127170. https://doi.org/10.1155/2013/127170

Zhao Y, Adjei AA. 2015. Targeting angiogenesis in cancer therapy: Moving beyond vascular endothelial growth factor. *The Oncologist* 20: 660–673.